Available online at www.sciencedirect.com

ScienceDirect

IFAC Papers Online CONFERENCE PAPER ARCHIVE

IFAC PapersOnLine 54-20 (2021) 108–113

Adaptive Parameter Estimation of a Steerable Drifter ⋆

Eric Gaskell * **Xiaobo Tan** **

* *Electrical and Computer Engineering Department, Michigan State University, East Lansing, MI 48824 USA (e-mail: gaskelle@msu.edu)*

** *Electrical and Computer Engineering Department, Michigan State University, East Lansing, MI 48824 USA (e-mail: xbtan@egr.msu.edu)*

Abstract: Steerable drifters are a promising energy-efficient environmental sampling platform for aquatic environments with pronounced flows, such as rivers and lakes or oceans with circulation structures. Due to aging and environmental variability, the dynamics of a drifter are often uncertain, which poses challenges in achieving desired control of the robot. In this paper online parameter estimation is explored for a drifter model that is highly nonlinear. With a gradient descent method, the convergence behavior of the adaptation law is explored for two different flow conditions, a parabolic flow and a uniform flow. The influence of the system input, the rudder angles, is also examined for two cases, fixed and sinusoidally varying. The region and speed of parameter convergence are studied in terms of the initial parameter estimate via simulation, which results in a number of findings. For example, for the parabolic flow setting, the region of convergence is much larger than that for the uniform flow setting, with a generally faster convergence, and varying the input results in faster convergence than holding the input constant. Furthermore, for each flow setting and input, there is a clear region of initial parameter estimates for which convergence is achieved more quickly than other parameter estimates. Convergence time is found to depend mostly on the distance of the initial parameter estimate from a trench in the parameter space. This could be useful for informing initial parameter estimates. The spectral content of the regressor is then examined to gain insight into the adaptive behavior.

Keywords: Marine robotics, steerable drifter, adaptive parameter estimation

1. INTRODUCTION

Engineers have sought to automatically monitor the quality of waterways and marine ecosystems since at least 1958, when Cleary (1958, 1962) first proposed and later developed a system of 6 stationary analyzers in the Ohio River Valley. A solution preferred over stationary analyzers is a drifting platform that can passively float and make measurements at multiple points in a waterway. Due to the necessity to tailor sensors to the waterway in order to establish cause-and-effect relationships with water quality, as discussed by Rickert and Hines (1978), a drifting platform could be outfitted with sensors selected to make various measurements of scientific interest. Drifters have been employed by Bishop et al. (2002, 2004) to measure the effect of natural and artificial iron fertilization on marine exosystems. Kieber et al. (1997) used free-floating drifters to measure light fluxes and photochemical processes in seawater. Because they are subject to drift wherever the current takes them, low-cost GPS tracked drifters have been used by Austin and Atkinson (2004) to take Lagrangian measurements of hydrodynamic forces.

The Argo Program is a collaborative, international effort that also uses a somewhat more advanced drifting sensor platform, as described by Roemmich et al. (2009). Argo floats drift underwater, making depth profiles of various measurements on a 10 day cycle. The Argo Program has, as of this writing, 30 member nations, each sharing data in an open data policy. Acoustic data from a modified Argo float has been used by Riser et al. (2008) to monitor rainfall and infer monsoon signals in the Bay of Bengal. Johnson et al. (2009) describes low-power sensors with a long operational lifespan, allowing the Argo program to collect massive amounts of data on a global scale, potentially for years. Like other drifters, Argo floats drift wherever currents take them, and take measurements at their current position. A steerable drifter has an advantage over current oceanographic technology, because it could have more control over its trajectory.

Gaskell and Tan (2020) proposed a steerable drifter and developed a dynamic model for its behavior. The proposed drifter can alter its trajectory somewhat by modulating hydrodynamic forces present on the rudders. While having an accurate model is important to the precise control and prediction of the drifter behavior, in practice the model parameters often have uncertainties due to material aging and variability in environmental conditions. It is thus of interest to estimate/update the model parameters in real time for precision control of steerable drifters.

In this paper adaptive parameter estimation is investigated for the steerable drifter model proposed by Gaskell and Tan (2020). A gradient descent approach for parameter es-

⋆ This work was supported by the National Science Foundation (IIS 1715714, IIS 1848945).

10.1016/j.ifacol.2021.11.161

timation, based on the position and velocity measurements of the drifter, is formulated. The speed of the adaptation is examined for constant and time-varying rudder angles and under two different types of environmental flows (parabolic flow and uniform flow). The convergence time is found to depend mostly on the distance of the initial parameter estimate from a trench visible in the parameter space. Along the trench, the adaptation occurs very quickly, but far from the trench, the adaptation occurs very slowly. Under the uniform flow, the adaptation often fails to converge, but does not fail for any initial estimate simulated under the parabolic flow. Furthermore, a sinusoidally varying rudder angle input is found to improve the adaptation speed under the parabolic flow, but appears to harm adaptation performance in the uniform flow. This conclusion is then supported by examining the frequency content of the regressor used for adaptation.

2. REVIEW OF THE DYNAMIC MODEL

Steerable drifters float in waterways and do not generate thrust. Instead, they exert limited control over their motion by adjusting the angles (and thus drag forces experienced by) of two or more rudders. The drifter modeled in this work is slightly modified from the configuration proposed by Gaskell and Tan (2020). A schematic of the drifter and model reference frames is shown in Fig. 1.

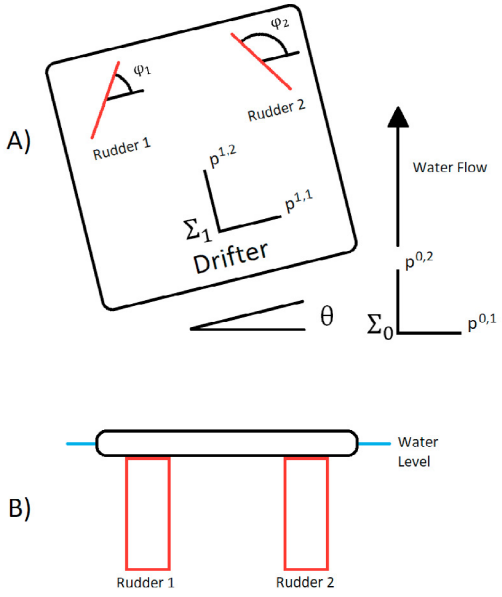

Fig. 1. A) Drifter rudder configuration, inertial reference frame Σ_0, and body-fixed reference frame Σ_1; B) rear view of the drifter.

Each rudder is assumed to rotate about the center of the rudder, and thus the center position of each rudder in the body-fixed frame, expressed as $r^1_{i,c}$ for rudder i, is constant. This does not affect the expressions for the dynamics of the proposed drifter as established by Gaskell and Tan (2020). The drifter is assumed to be constrained to planar motion at the surface of the water. It is also assumed that drag on the body of the drifter would be negligible compared to the drag on the panels. For the purposes of analysis, rudder angles are assumed quasi-static.

The drifter can be viewed as modulating the potential drag force on each rudder. Each rudder experiences a drag force in the direction of the relative velocity of the water, proportional to the square of the relative velocity, and proportional to the wetted area. By changing the rudder angle, the drifter can control the wetted area, and thus adjust the magnitude of the force seen by each rudder.

The rotation matrix R^0_1 between the body-fixed frame and the inertial frame shown in Fig. 1 is given by

$$R^0_1 = \begin{bmatrix} \cos(\theta) & -\sin(\theta) \\ \sin(\theta) & \cos(\theta) \end{bmatrix} \tag{1}$$

where θ is the angle between the body-fixed frame and the inertial frame. The relative velocity $v^0_{i,r}$ of rudder i to the flow in the inertial frame is then:

$$v^0_{i,r} = v^0_{i,c} - v^0_{i,f} = \frac{d}{dt}[p^0] + \begin{bmatrix} 0 & 1 \\ -1 & 0 \end{bmatrix} R^0_1 r^1_{i,c} \frac{d}{dt}[\theta] - v^0_{i,f} \tag{2}$$

where $v^0_{i,c}$ is the velocity of the center of rudder i in the inertial frame, $v^0_{i,f}$ is the velocity of the water at the center of rudder i in the inertial frame, p^0 is the position of the center of mass of the drifter in the inertial frame, and $r^1_{i,c}$ is the position vector of rudder i in the body-fixed frame. The relative velocity in the inertial frame is related to the relative velocity in the body-fixed frame through the rotation matrix R^0_1 as follows:

$$v^0_{i,r} = R^0_1 v^1_{i,r} \tag{3}$$

where $v^1_{i,r}$ is the velocity of rudder i relative to the flow in the body-fixed frame. Note that

$$\|v^0_{i,r}\| = \|v^1_{i,r}\| \tag{4}$$

where $\|\cdot\|$ is the L^2-norm. Equations (5) and (6) below capture the linear and rotational dynamics of the drifter, respectively:

$$\frac{d^2}{dt^2}p^0 = -\frac{c_d\rho}{2m} R^0_1 \left[A_1 |\sin\left(\angle v^1_{1,r} - \phi_1\right)| \|v^1_{1,r}\| v^1_{1,r} + A_2 |\sin\left(\angle v^1_{2,r} - \phi_2\right)| \|v^1_{2,r}\| v^1_{2,r}\right] \tag{5}$$

$$\frac{d^2}{dt^2}\theta = -\frac{c_d\rho}{2I}\left[A_1 |\sin\left(\angle v^1_{1,r} - \phi_1\right)| \|v^1_{1,r}\| \left(v^1_{1,r}\right)^T \begin{bmatrix} 0 & 1 \\ -1 & 0 \end{bmatrix} r^1_{1,c} + A_2 |\sin\left(\angle v^1_{2,r} - \phi_2\right)| \|v^1_{2,r}\| \left(v^1_{2,r}\right)^T \begin{bmatrix} 0 & 1 \\ -1 & 0 \end{bmatrix} r^1_{2,c}\right] \tag{6}$$

where $\angle$ denotes the angle of a vector, ϕ_1, ϕ_2 are the rudder angles as seen in Fig 1, c_d is the drag coefficient of the rudders, ρ is the fluid density, m is the drifter's added mass, I is the drifter's added moment of inertia, and A_i is the area of rudder i.

The physical drifter parameters can be collected into a single term for each rudder, β_i, as follows:

$$\beta_i = -\frac{c_d \rho A_i}{2m} \tag{7}$$

Define angle-of-attack α_i as

$$\alpha_i = \angle v^1_{i,r} - \phi_i \tag{8}$$

For a 2-rudder drifter, the translational dynamics can then be expressed as

$$\frac{d^2}{dt^2}p^0 = \big[\beta_1 |\sin\alpha_1| \|v^0_{1,r}\| v^0_{1,r} + \beta_2 |\sin\alpha_2| \|v^0_{2,r}\| v^0_{2,r}\big] \tag{9}$$

3. ADAPTIVE PARAMETER ESTIMATION

This section outlines the formulation of an adaptive parameter estimator for the drifter model parameter β_i, $i = 1, 2$. Equation (9) can be rewritten as

$$\frac{d^2}{dt^2}p^0 = \big[|\sin\alpha_1| \|v^0_{1,r}\| v^0_{1,r}, |\sin\alpha_2| \|v^0_{2,r}\| v^0_{2,r}\big] \begin{bmatrix}\beta_1 \\ \beta_2\end{bmatrix} \tag{10}$$

where β_1 and β_2 are assumed to be unknown. It is assumed that the drifter's position and velocity, but not acceleration, are available. Define a polynomial $\Lambda(s)$

$$\Lambda(s) = s^2 + \lambda_1 s + \lambda_2 \tag{11}$$

where $\lambda_1, \lambda_2 > 0$ and s represents the Laplace variable. One can then rewrite equation (10) using the hybrid time-domain and Laplace-domain notation described by Tao (2003):

$$\frac{s^2}{\Lambda(s)}p^0 = \frac{1}{\Lambda(s)}\big[|\sin\alpha_1| \|v^0_{1,r}\| v^0_{1,r}, |\sin\alpha_2| \|v^0_{2,r}\| v^0_{2,r}\big] \begin{bmatrix}\beta_1 \\ \beta_2\end{bmatrix} \tag{12}$$

To follow the nomenclature convention for the gradient descent algorithm we define

$$y = \frac{s^2}{\Lambda(s)}p^0$$

$$\Phi^T = \frac{1}{\Lambda(s)}\big[|\sin\alpha_1| \|v^0_{1,r}\| v^0_{1,r}, |\sin\alpha_2| \|v^0_{2,r}\| v^0_{2,r}\big] \tag{13}$$

$$\Theta^* = \begin{bmatrix}\beta_1 \\ \beta_2\end{bmatrix} \tag{14}$$

With these definitions, the system can be expressed as

$$y = \Phi^T \Theta^* \tag{15}$$

These definitions view the filtered position of the drifter as the system output, and express it as a product of a regressor matrix Φ with a vector of unknown quantities Θ^*.

Because Θ^* consists of unknown values β_1 and β_2, the predicted system output $\hat{y}$ cannot use these values. Instead, $\hat{y}$ is formed from the current estimate of these parameters, Θ, as follows:

$$\hat{y} = \Phi^T \Theta \tag{16}$$

Defining the error

$$\epsilon = \hat{y} - y \tag{17}$$

One can apply the gradient descent algorithm to estimate Θ:

$$\dot{\Theta} = -\frac{\Gamma \Phi \epsilon}{k^2} \tag{18}$$

where $\Gamma \in \mathbb{R}^{2\times 2}$ is the adaptive gain, and k is a normalizing factor defined as

$$k = \sqrt{1 + \|\Phi\|^2} \tag{19}$$

Defining Θ_0 as an initial estimate of the true parameters Θ^*, one can obtain the current estimate of Θ at time t:

$$\Theta(t) = \Theta_0 + \int_{t_0}^{t} \dot{\Theta} \mathrm{d}t \tag{20}$$

Typical applications of the gradient descent algorithm use a regressor vector to estimate the unknown parameters. The regressor matrix Φ given by equation (13) is composed of two such vectors, corresponding to the two position components, respectively. The resultant adaptation $\dot{\Theta}$ is the sum of the adaptations in both directions. This is thought to provide a more robust parameter estimator because if either scalar adaptation would achieve convergence, then the vector adaptation should as well.

4. SIMULATION RESULTS

The highly nonlinear dynamics of the drifter poses significant challenges in predicting the adaptation behavior. In this section simulation is conducted for different rudder (system input) settings and ambient flow conditions to gain insight into parameter convergence properties of the proposed parameter estimation algorithm. Table 1 lists the physical parameters used in the simulation.

Table 1. Simulation parameters.

c_d	1.2
ρ	1000 kg/m^3
m	15 kg
I	2.5 kg m^2
A_1	0.105 m^2
A_2	0.095 m^2

The dynamic model for the drifter is simulated in a simplified model of a river with two different flow profiles, a parabolic flow and a uniform flow. The parabolic flow profile, illustrated in Fig. 2, achieves a maximum velocity

of 0.68 m/s in the center, and is 4 meters wide. For both the uniform and parabolic flow profiles, the river is modeled as perfectly straight.

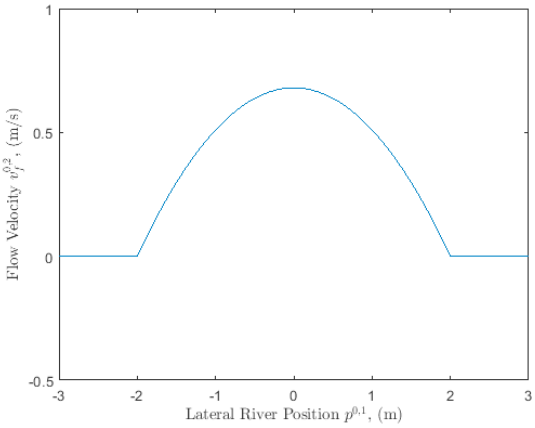

Fig. 2. Illustration of parabolic flow: longitudinal river flow velocity vs. lateral drifter position in river.

For all cases simulated, the drifter is started at position $p^0 = [0, 0]^T$, with an initial velocity of $\frac{d}{dt}p^0 = [0, 0]^T$ and an initial angular velocity of $\omega = 0$.

The true value of Θ^* can be calculated from the physical parameters:

$$\Theta^* = \begin{bmatrix}\beta_1 \\ \beta_2\end{bmatrix} = \begin{bmatrix}-4.2 \\ -3.8\end{bmatrix} \tag{21}$$

An important question is the region of attraction for the initial parameter estimate. For this study, we consider the range of initial parameter estimate as

$$\beta_1 \in [-3.7, -4.7] \tag{22}$$
$$\beta_2 \in [-3.3, -4.3] \tag{23}$$

The adaptation gain matrix is selected as:

$$\Gamma = 5 \times 10^5 I_2 \tag{24}$$

where I_2 is the 2-dimensional identity matrix. The filter polynomial $\Lambda(s)$ is chosen as

$$\Lambda(s) = s^2 + s + 1 \tag{25}$$

First, the drifter is simulated with constant rudder angles ϕ equal to:

$$\phi = \begin{bmatrix}\frac{\pi}{2} - 0.1 \\ \frac{\pi}{2} + 0.1\end{bmatrix} \tag{26}$$

These rudder angles are chosen as they drive the drifter in a stable trajectory described by Gaskell and Tan (2020), and present a small initial angle of attack on both panels. With a small angle of attack, the drifter takes longer to catch up to the speed of the river, which is beneficial for improving the excitation level of the regressors. Once the drifter's velocity approaches that of the river, no rudder angle will change the drifter's acceleration, and thus no information can be gained for adaptation. Convergence time is defined as the minimum time t_1 such that:

$$\|\Theta^* - \Theta\| < 0.01 \tag{27}$$

If the system does not achieve convergence within 30 seconds, the adaptation is considered a failure. Analysis of the frequency content of the regressor suggests that adaptation will either occur earlier than this, or is unlikely to occur.

4.1 Adaptation Under Parabolic Flow

The steerable drifter system is first simulated under each input case in a parabolic flow.

Initial estimates for β_1, β_2 are selected as an evenly spaced 101×101 grid spanning the ranges given by Eqs. (22) and (23). The convergence times are then found for each initial estimate of β_1, β_2, and plotted in Fig. 3.

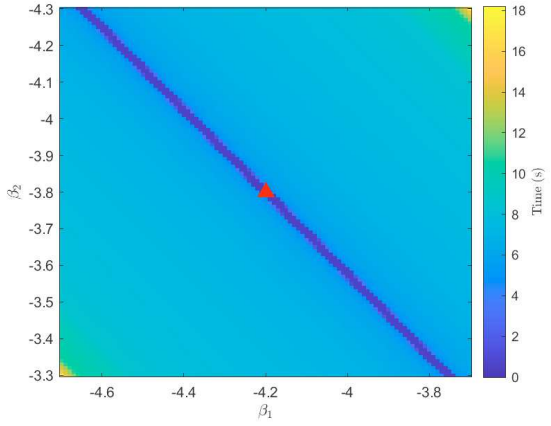

Fig. 3. Map of convergence time vs. initial parameter estimate for constant rudder angles in a parabolic flow, where the true parameter values are marked with a triangle.

The mean time to converge under these conditions over the selected β_1, β_2 is found to be 6.98 seconds.

Simulation is then conducted with the same parameters but under the following oscillatory rudder angles:

$$\phi = \begin{bmatrix}\frac{\pi}{2} - 0.1 + 0.1\sin(t) \\ \frac{\pi}{2} + 0.1 + 0.1\sin(2t)\end{bmatrix} \tag{28}$$

The extra sinusoidal variation in ϕ_1, ϕ_2 is chosen to add to the frequency content of the control input.

The time to converge under sinusoidally varying input is then plotted in Fig. 4. For sinusoidally varying rudder angles over the selected β_1, β_2, the mean time to converge is found to be 5.71 seconds.

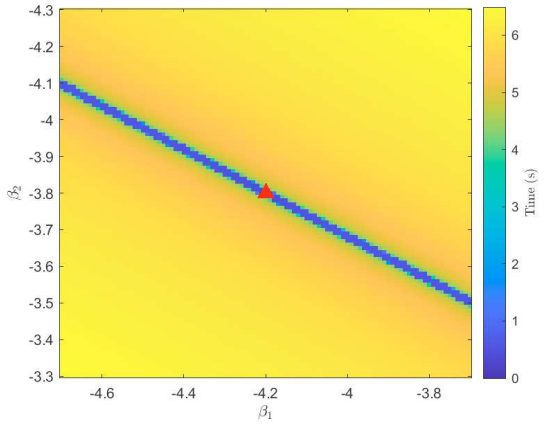

Fig. 4. Map of convergence time vs. initial parameter estimate for sinusoidally varying rudder angles in a parabolic flow, where the true parameter values are marked with a triangle.

4.2 Adaptation Under Uniform Flow

The steerable drifter system is then simulated under each input case in a uniform flow with velocity of 0.34 m/s. This is chosen as half of the peak velocity of the parabolic flow profile, and is meant to approximate a wide, slow river.

Under the uniform flow, for many initial estimates, the parameter estimate fails to converge within the allowed time (30 s). For initial estimates that do result in parameter convergence, the convergence times are plotted in Fig. 5 for constant rudder angles and Fig. 6 for sinusoidally varying rudder angles. Due to the large regions where parameter adaptation fails to converge, the mean convergence times under uniform flow are not plotted.

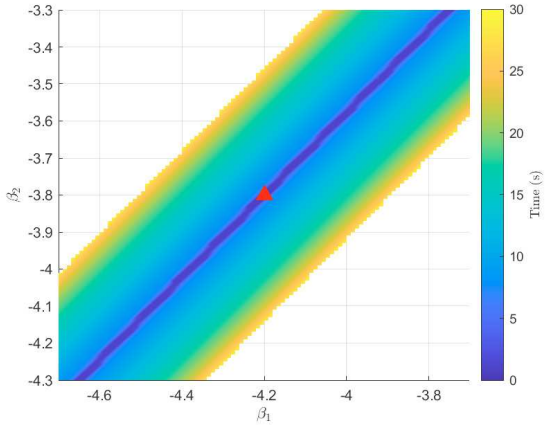

Fig. 5. Map of convergence time vs. initial parameter estimate for constant rudder angles in a uniform flow, where the true parameter values are marked with a triangle.

For all cases simulated, there is a clear pattern to the data. On average, under the parabolic flow, varying the rudder angles results in parameter convergence 1.27 seconds faster. However, under the uniform flow, sinusoidally varying the input dramatically reduces the region in initial parameter estimate for which convergence is achieved. For

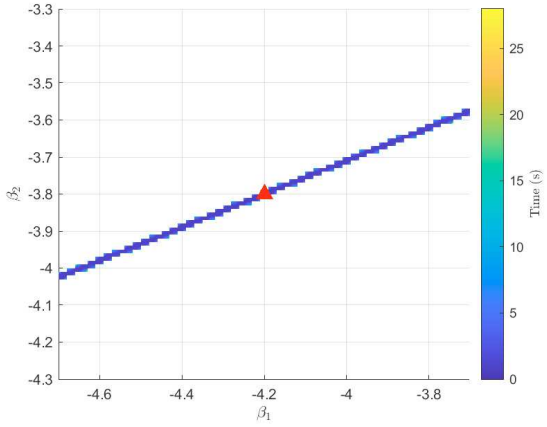

Fig. 6. Map of convergence time vs. initial parameter estimate for sinusoidally varying rudder angles in a uniform flow, where the true parameter values are marked with a triangle.

all cases, there is a clear trench in the parameter space, passing through the true values, where the convergence time is significantly faster than other regions. For the constant rudder angle inputs under the parabolic flow, there are also regions of extremely slow convergence in the corners farthest from this trench.

4.3 Spectral Analysis of the Regressor

In order to gain insight into the behavior of this adaptive system, spectral analysis is performed on the contents of the regressor. The frequency content is evaluated against time for each element of the regressor matrix using a sliding window of 10 s. Fig. 7 illustrates the frequency content of Φ_{22} for each input and flow case. It is interesting to note that, due to the highly nonlinear dynamics, the regressor signals contain a rich spectrum even under constant rudder angles. This explains why the parameter estimate converges in most cases despite the seemingly "unexciting" inputs.

For each input and flow case, the regressor has a rich spectrum of frequencies at the beginning that quickly fades by around $t = 10s$, and the spectral plots each have a similarly banded structure. Under the parabolic flow, the peaks of the spectra are higher than those under the uniform flow. Furthermore, under the parabolic flow, sinusoidally varying the input seems to sharpen the peaks of the spectrum over a constant input. However, varying the input under the uniform flow caused the frequency spectrum to decay faster, without significantly enriching the spectrum.

Because the drifter primarily drifts with the river in the $p^{0,2}$ direction, the spectra of $\Phi_{1,2}, \Phi_{2,2}$ have a greater magnitude than the spectra of $\Phi_{1,1}, \Phi_{2,1}$. This suggests that adaptation could be performed along this direction only, to reduce computational complexity.

5. CONCLUSION

In this paper parameter estimation for a steerable drifter was studied under a gradient descent adaptation scheme.

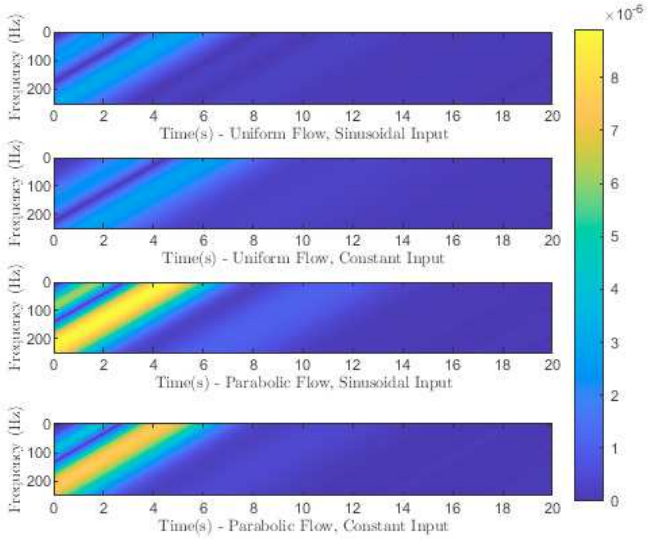

Fig. 7. Frequency spectrum vs. time for Φ_{22} under each flow and input case.

In particular, the parameter convergence behavior under different combinations of flow conditions and rudder inputs was explored via simulation, where the regions of attraction for the initial parameter estimate were studied.

A trench was identified in the plots of convergence time for each case. If the initial parameter estimate was close to this trench, the adaptation would occur very rapidly. If the initial parameter estimate was too far from this trench, the adaptation would take significantly longer or fail to converge. This information may prove useful for informing initial guesses for unknown parameters. A bias term may be added to the initial guess to avoid regions of slow convergence, or move toward regions of rapid convergence.

It was found that convergence was more reliable under a parabolic flow than a uniform flow. It was also found that for a parabolic flow, adding an oscillatory term to the input improved the adaptation. However, under a uniform flow, a varying input hurt the adaptive performance.

The spectrum of the regressor was then analyzed over time. It was found that under a uniform flow, varying the input caused the spectrum to decay faster without significantly enriching the regressor. However, under a parabolic flow, varying the input enriched the regressor enough to improve the adaptive performance. It was also found that elements of the regressor corresponding to the drifter's longitudinal position in the river were much greater than elements corresponding to the lateral position. This suggests that longitudinal position may be used for adaptation alone, without lateral position, to reduce computational complexity.

We note from the spectral analysis of the regressors that the regressors under drifting tend to zero within finite time, which motivates faster adaptation algorithms. Part of our future work involves the exploration of accelerated learning algorithms (see, e.g., Gaudio et al. (2020)) for this problem. In addition, the adaptive parameter estimation proposed in this work is the first step toward designing an adaptive control scheme, which we are also pursuing. Because of the nonlinearities present in the drifter model, the work by Kanellakopoulos et al. (1992) in designing controllers that avoid hard nonlinearities is of particular interest. Finally, we plan to experimentally verify the adaptive estimation and control methods on a steerable drifter prototype.

REFERENCES

Austin, J. and Atkinson, S. (2004). The design and testing of small, low-cost GPS-tracked surface drifters. *Estuaries*, 27(6), 1026–1029.

Bishop, J.K.B., Davis, R.E., and Sherman, J.T. (2002). Robotic observations of dust storm enhancement of carbon biomass in the North Pacific. *Science*, 298(5594), 817–821.

Bishop, J.K.B., Wood, T.J., Davis, R.E., and Sherman, J.T. (2004). Robotic observations of enhanced carbon biomass and export at 55°s during SOFeX. *Science*, 304(5669), 417–420.

Cleary, E.J. (1958). Development of a robot system. *Journal AWWA*, 50(9), 1219–1222.

Cleary, E.J. (1962). Robot monitor system for the ohio valley. *Journal AWWA*, 54(11), 1347–1352.

Gaskell, E. and Tan, X. (2020). Dynamic modeling of a steerable drifter. volume Volume 2 of *2020 ASME Dynamic Systems and Control Conference*. URL `https://doi.org/10.1115/DSCC2020-3295`. V002T28A003.

Gaudio, J.E., Annaswamy, A.M., Moreu, J.M., Bolender, M.A., and Gibson, T.E. (2020). Accelerated learning with robustness to adversarial regressors. URL `https://arxiv.org/abs/2005.01529`.

Johnson, K.S., Berelson, W.M., Boss, E.S., Chase, Z., Claustre, H., Emerson, S.R., Gruber, N., Kortzinger, A., Perry, M.J., and Riser, S.C. (2009). Observing biogeochemical cycles at global scales with profiling floats and gliders: Prospects for a global array. *Oceanography*, 22(3), 216–225.

Kanellakopoulos, I., Krstic, M., and Kokotovic, P.V. (1992). Interlaced controller-observer design for adaptive nonlinear control. In *1992 American Control Conference*, 1337–1342. doi:10.23919/ACC.1992.4792321.

Kieber, D.J., Yocis, B.H., and Mopper, K. (1997). Free-floating drifter for photochemical studies in the water column. *Limnology and Oceanography*, 42(8), 1829–1833.

Rickert, D.A. and Hines, W.G. (1978). River quality assessment: Implications of a prototype project. *Science*, 200(4346), 1113–1118.

Riser, S.C., Nystuen, J., and Rogers, A. (2008). Monsoon effects in the bay of bengal inferred from profiling float-based measurements of wind speed and rainfall. *Limnology and Oceanography*, 53(5), 2080–2093.

Roemmich, D., Johnson, G.C.J.G.C., Riser, S., Davis, R.D.R., Gilson, J., Owens, W.B., Garzoli, S.L., Schmid, C., and Ignaszewski, M. (2009). The argo program: Observing the global ocean with profiling floats. *Oceanography*, 22(2), 34–43.

Tao, G. (2003). *Adaptive control design and analysis*. Wiley IEEE Press Imprint.